Available online at www.sciencedirect.com
ScienceDirect
Tetrahedron: Asymmetry
Tetrahedron: *Asymmetry* 18 (2007) 1521–1528

Circular dichroism spectra of *trans*-chalcone epoxides

Krisztina Pál,[a] Mihály Kállay,[b] Miklós Kubinyi,[a,b,*] Péter Bakó[c] and Attila Makó[c]

[a]*Institute of Structural Chemistry, Chemical Research Center, Hungarian Academy of Sciences, PO Box 17, 1525 Budapest, Hungary*
[b]*Department of Physical Chemistry, Budapest University of Technology and Economics, 1521 Budapest, Hungary*
[c]*Department of Organic Chemical Technology, Budapest University of Technology and Economics, 1521 Budapest, Hungary*

Received 9 March 2007; revised 23 June 2007; accepted 28 June 2007

Abstract—The electronic absorption and CD spectra of (−)-*trans*-chalcone epoxide and its derivatives with methyl and alkoxy substituents at the *ortho*-positions of the aromatic rings have been measured. The spectra have been assigned with help of the energies, oscillatory strengths, and rotatory strengths of the singlet transitions obtained from DFT calculations. The features of the CD spectra, indicative of the absolute configuration, are the carbonyl n–π* band and two further strong bands assigned to the overlapping signals of π–π* and n_{epoxy}–π* excitations.

1. Introduction

The catalytic epoxidation of chalcone, leading to *trans*-chalcone epoxide has been used many times for characterizing the enantioselectivity of various types of chiral catalysts.[1a–k] In several cases, the scope of the studies was extended to substituted chalcones.[2a–f] Chiral chalcone epoxides are also of great importance as intermediates for the synthesis of natural products and pharmaceuticals, primarily enantiomeric flavonoid monomers.[3a–e]

The absolute configuration of chalcone epoxide was deduced by chemical correlation,[4] and the absolute configurations of some derivatives were determined by single crystal X-ray diffraction[2d] and CD spectroscopy.[2d,f,3b,d] The assignment of the CD spectra of *trans*-chalcone epoxides has so far been restricted to the band belonging to the n–π* transition of the carbonyl group. Herein, we undertook the analysis of the CD spectra of *trans*-chalcone epoxide **3** and its substituted derivatives **3a**–**e** (see Scheme 1), involving the lower wavelength range of the spectra, where the bands associated with the π–π* transitions of the phenyl and benzoyl groups are expected. Our aim has been to identify the features of the CD spectra, which are indicative of the absolute configurations of such molecules.

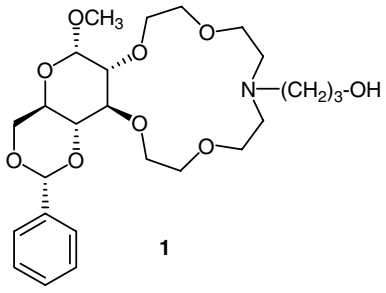

1

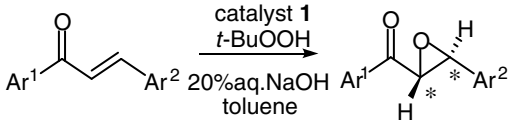

2a-e **3, 3a-e**

3	$Ar^1 = Ar^2 = Ph$
2a, 3a	$Ar^1 = 2\text{-}CH_3\text{-}Ph$, $Ar^2 = Ph$
2b, 3b	$Ar^1 = 2\text{-}CH_3O\text{-}Ph$, $Ar^2 = Ph$
2c, 3c	$Ar^1 = 2\text{-}EtOCH_2O\text{-}Ph$, $Ar^2 = Ph$
2d, 3d	$Ar^1 = 2\text{-}CH(CH_3)_2O\text{-}Ph$, $Ar^2 = Ph$
2e, 3e	$Ar^1 = Ph$, $Ar^2 = 2\text{-}CH_3\text{-}Ph$

Scheme 1. The enantioselective epoxidation of chalcones.

* Corresponding author. Tel.: +36 1 438 1120; fax: +36 1 438 1143; e-mail: kubinyi@mail.bme.hu

0957-4166/$ - see front matter © 2007 Elsevier Ltd. All rights reserved.
doi:10.1016/j.tetasy.2007.06.034

The CD spectra of various chalcone epoxides with substituents in the *para*-position of their aromatic rings have been published in our previous papers.[2d,f] The present study concerns, primarily the substituent effects on the CD spectrum of chalcone epoxide caused by substituents at the *ortho*-positions of its aromatic rings.

To achieve a reliable assignment of the spectra, quantum chemical calculations were carried out to yield the equilibrium geometries, and the characteristics of the electronic absorption and CD spectra. Whereas the calculations of molecular geometries and absorption spectra are nowadays well established, the computation of chiroptical spectra still remains a difficult task. In recent years, significant progress has been made in this field. Currently, implementations are available at the semi-empirical level,[5] for the ab initio configuration interaction singles (CIS) and random phase approximation (RPA) methods,[6a,b] the multireference configuration interaction (MRCI),[7a–c] coupled cluster (CC),[8a–d] and time-dependent density functional theory (TD-DFT)[9a–f] approaches. Very recently, the inclusion of vibrational effects in the calculation of CD spectra has been considered and found to be vital in certain cases.[10] It has also been demonstrated that the vibronic coupling can have additional, unusually strong effects on the CD spectrum.[11]

2. Results and discussion

2.1. Synthesis of chalcone epoxides

The chiral *trans*-epoxyketones **3a**–**e** were synthesized by the enantioselective epoxidation of the corresponding *trans*-chalcones **2a**–**e** with *tert*-butylhydroperoxide using a phase transfer catalyst, the chiral crown ether **1**,[2d] (Scheme 1). The preparations of **3a**, **3b**, and **3e** using alternative methods for the enantioselective epoxidation of *trans*-chalcones were reported in the literature,[12a–c] whereas **3c** and **3d** are novel compounds.

The requisite *trans*-(*E*)-chalcones having a methyl- or methoxy group **2a** and **2b** were obtained by base-catalyzed condensation of benzaldehyde with 2′-methyl acetophenone[13] or 2′-methoxy acetophenone,[14] respectively. The reaction of acetophenone with *ortho*-tolualdehyde[15] gave compound **2e**. Preparation of the novel analogues substituted with an ethoxymethyl group ($EtOCH_2O$) **2c** and **2d** having an isopropyl group were performed in two steps (Scheme 2).

2′-Hydroxyacetophenone **4** was treated with chloromethyl ethyl ether in a mixture of aq potassium hydroxide and dichloromethane in the presence of tricaprylylmethyl ammonium chloride[3b] to give compound **5c** after column chromatography with a yield of 47%. We obtained 2′-isopropoxyacetophenone **5d** in the reaction of compound **4** with isopropyl bromide (K_2CO_3, KI) in acetone[16] with a yield of 32%. The condensation of the substituted acetophenones **5c** and **5d** with benzaldehyde gave chalcone derivatives **2c** (67%) and **2d** (59%), respectively.

The epoxidation of chalcones with *tert*-butylhydroperoxide (TBHP, 2 equiv) was carried out in a liquid–liquid two-phase system in toluene, employing 20% aq NaOH (3.5 equiv) as the base and 7 mol % of chiral crown catalyst **1** at a temperature of 2–5 °C (Scheme 1). After the usual work-up procedure, the product was isolated by preparative TLC. The asymmetric induction, expressed in terms of the enantiomeric excess (ee), was monitored by ^1H NMR analysis using (+)-Eu(hfc)$_3$ as a chiral shift reagent. The *trans*-epoxyketones **3a**–**e** were formed in all experiments with excesses of the enantiomers with negative specific rotations. Table 1 summarizes the results obtained

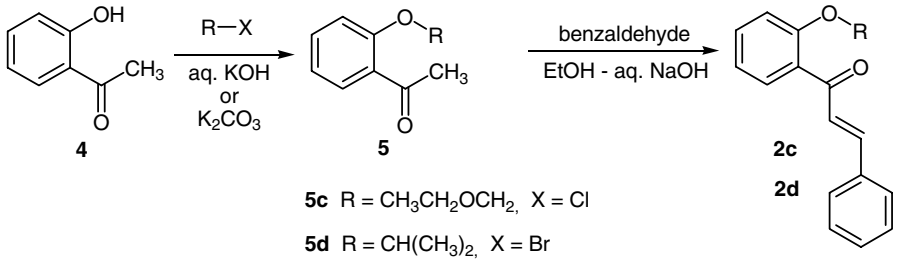

Scheme 2.

Table 1. Epoxidation of substituted chalcones by *t*-BuOOH in the presence of catalyst **1** at 2–5 °C

Chalcones	Ar^1	Ar^2	Epoxides	Time (h)	Yield[a] (%)	$[\alpha]_D$[b]	ee[c] (%)
2a	2-CH_3–Ph	Ph	**3a**	4	52	−166.9	71
2b	2-CH_3O–Ph	Ph	**3b**	8	49	−98.5	83
2c	2-$EtOCH_2O$–Ph	Ph	**3c**	8	46	−102.3	70
2d	2-$CH(CH_3)_2O$–Ph	Ph	**3d**	12	53	−131	79
2e	Ph	2-CH_3–Ph	**3e**	4	55	−75.7	76

[a] Based on isolation by preparative TLC.
[b] In CH_2Cl_2 at 22 °C.
[c] Determined by ^1H NMR spectroscopy in the presence of Eu(hfc)$_3$ as a chiral shift reagent.

with the differently substituted ketones. As can be seen, the yields are between 46% and 55%, the enantioselectivities are significant (70–83% ee) and do not depend much on the substituent on the aromatic ring.

2.2. Quantum chemical calculations

In order to reveal the effect of substitution on the CD spectra, quantum chemical calculations have been performed for (−)-**3** and for two methyl and one methoxy derivatives, **3a**, **3b**, and **3e**.

First, a conformational analysis was carried out for **3** based on molecular mechanics calculations employing the MMFF94 force field[17] and simulated annealing algorithm. Molecular mechanics calculations were carried out by the SPARTAN'02 package.[18] The analysis concluded that two low-lying conformers existed. In the case of the lower-energy conformer, the phenyl rings are approximately at a right angle to one another, while they are roughly coplanar for the other conformer. In order to determine the accurate energy difference between the two conformers, geometry optimizations were performed at the second-order Møller–Plesset (MP2) level using the resolution of identity approximation (RI)[19] and the TZPP basis set.[20] The MP2 calculations were performed by the TURBOMOLE package.[21] The results of the MP2 calculations suggest that the first conformer is about 6 kJ/mol more stable than the other one, which means that about 90% of the molecules are twisted at room temperature. As a result the calculations were restricted to the twisted form of the compounds. The molecular geometries for the lowest-energy conformers of the substituted derivatives have been optimized with the aid of density functional theory (DFT) using the Becke 3-parameter-Lee–Yang–Parr (B3LYP) functional[22a,b] and Pople's 6-311++G**-basis set.[23]

After the geometry optimization, the absorption and CD spectra of the compounds have been calculated with a time-dependent DFT (TD-DFT) method[24] using the above functional and basis set. The rotatory strengths have been calculated in the velocity gauge, which guarantees the gauge origin independence of the calculated rotatory strengths. For the treatment of the solvent effects, in a further calculation the polarized continuum model (PCM)[25a,b] method was used with ethanol as the solvent. The calculations have been carried out by the GAUSSIAN 03 suite of quantum chemical programs.[26]

2.3. UV–vis absorption spectra

The UV–vis absorption and CD spectra of the unsubstituted compound **3** can be seen in Figure 1, where the theoretically calculated electronic transitions are also marked. The absorption spectrum of **3** is compared to those of its derivatives **3a**–**e** in Figure 2. The data of the observed UV and CD spectra of **3**, **3a**, **3b**, and **3e** are listed in Table 2, together with the wavelengths, oscillator strengths, and rotatory strengths obtained in the quantum chemical calculations for the isolated molecules. The calculations carried out with the PCM method indicated that the solvent effects are insignificant, for example, the theoretically estimated solvent shifts fell between 1 and 15 nm.

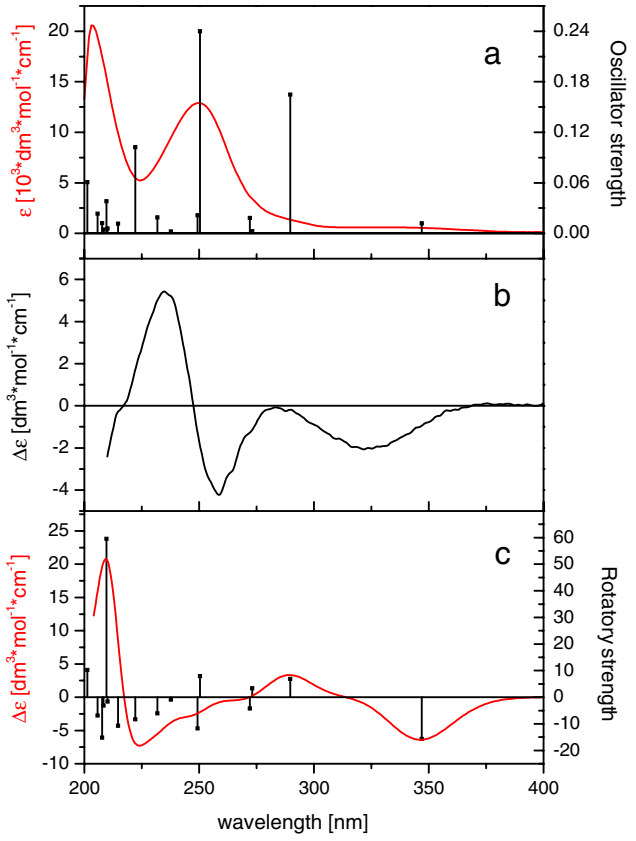

Figure 1. Experimental and calculated spectra of *trans*-chalcone epoxide (−)-**3**: (a) UV absorption spectrum and calculated oscillator strengths, (b) experimental CD spectrum, (c) calculated rotatory powers and CD spectrum.

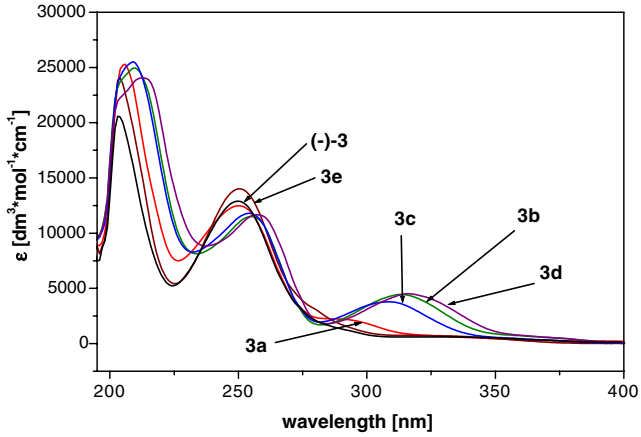

Figure 2. Absorption spectrum of *trans*-chalcone epoxide (−)-**3** and its derivatives **3a**–**e**.

2.3.1. Spectrum of *trans*-chalcone epoxide 3. The spectrum of **3** (see Fig. 1a) can be assigned with help of the calculated molecular orbitals, which are displayed in Figure 3 and of the TD-DFT vector coefficients characterizing the

Table 2. The data of the observed UV and CD spectra of **3**, **3a**, **3b**, and **3e**, together with the wavelengths, oscillator strengths and rotatory strengths obtained in the quantum chemical calculations

Compound	Observed		Calculated
	UV spectra λ_{max} [nm] (ε [M^{-1} cm^{-1}])	CD spectra λ_{max} [nm] ($\Delta\varepsilon$ [M^{-1} cm^{-1}])	Electronic transitions λ [nm] (osc. strength) {rot. strength}
3	330 (600)	324 (−2.007)	347 (0.012) {−15.7}
	290 sh		290 (0.165) {+6.8}
	275 sh		273 (0.003) {+3.3}
			272 (0.018) {−4.2}
		258 (−4.229)	250 (0.239) {+7.9}
	250 (12,900)		249 (0.021) {−11.7}
		235 (+5.425)	
	203 (20,590)		
3a	335 sh (600)	323 (−2.190)	346 (0.010) {−20.7}
	295 sh (2000)		285 (0.208) {−9.1}
			281 (0.017) {+0.9}
			266 (0.002) {−0.7}
		257 (−2.990)	250 (0.171) {+29.5}
	250 (12,500)		244 (0.009) {−12.1}
		234 (+4.035)	
	205 (25,200)		
3b	360 sh		349 (0.014) {−17.9}
	313 (4460)	308 (−4.402)	308 (0.150) {−9.8}
	270 sh		276 (0.112) {−2.7}
			260 (0.002) {−1.1}
		265 (−1.877)	248 (0.075) {+23.5}
	255 (11,500)		240 (0.008) {−7.8}
		237 (+8.021)	
	210 (24,060)		
3e	332 (700)	324 (−1.841)	345 (0.002) {−4.2}
	290 sh		298 (0.018) {−2.4}
	282 (2790)	279 (+1.944)	282 (0.023) {+3.6}
	270 sh		271 (0.017) {+3.6}
		259 (−1.687)	258 (0.008) {−12.5}
	250 (14,020)		250 (0.319) {−5.6}
		239 (+4.151)	
	204 (24,060)		

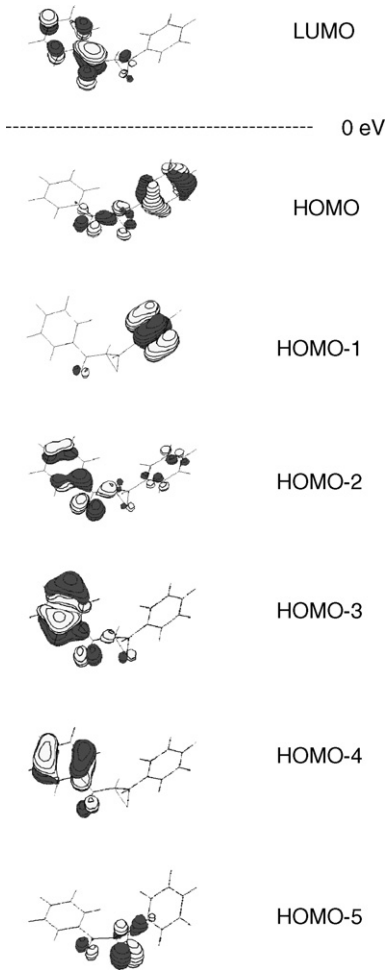

Figure 3. Molecular orbitals involved in the six lowest-energy transitions of compound **3**. The transitions are: (1) (HOMO)→(LUMO), (2) (HOMO−2)→(LUMO), (3) (HOMO−1)→(LUMO), (4) (HOMO−3)→(LUMO), (5) (HOMO−4)→(LUMO), and (6) (HOMO−5)→(LUMO).

contributions of the individual single electron promotions to the excited-state wave functions (not given here).

It is a common feature of the lowest-energy transitions that they all involve the LUMO as the unoccupied orbital, the excitations to LUMO+1 start at relatively high energies. The LUMO can be considered as the π^* orbital of the carbonyl moiety, π^*_{CO}.

The weak band at 330 nm belongs to the lowest-energy transition, which is a mixture of the HOMO→LUMO and the HOMO−2→LUMO single electron promotions. Empirically this band would be described as a carbonyl n→π^* transition. In fact, by the calculations none of the occupied MO-s can be visualized as a 'clear' n-orbital of the carbonyl oxygen, O1. In the HOMO the n_{O1} orbitals are combined with the π orbitals of Ph2, the phenyl group attached to the epoxy ring, in the HOMO−2 they are combined with the π orbitals of Ph1, the phenyl group of the benzoyl moiety, thus this transition has a mixed $n_{O1} \rightarrow \pi^*_{CO}$, $\pi_{Ph1} \rightarrow \pi^*_{CO}$, $\pi_{Ph2} \rightarrow \pi^*_{CO}$ character. The shoulder at 290 nm corresponds to another combination of the HOMO→LUMO and HOMO−2→LUMO excitations.

The strong band at 250 nm probably covers at least four electronic transitions. The weak shoulder at around 275 nm can be assigned to the 3rd and 4th transitions in Table 2 (in order of increasing energy), which are nearly degenerate and have $\pi_{Ph} \rightarrow \pi^*_{CO}$ character. For the 3rd transition the HOMO−1→LUMO excitation is predominant, while in the other the HOMO−3→LUMO is predominant. The HOMO−1 and HOMO−3 are π orbitals of the two benzene rings, by shape they are the analogues of the HOMOs of toluene[27] and benzaldehyde,[28] respectively. The peak at 250 nm also seems to be associated with two closely lying transitions. One of them, the 5th in Table 2, is dominated by the HOMO−4→LUMO, the other (6th in Table 2) by the HOMO−5→LUMO single electron promotion. The HOMO−4 is a π orbital of the Ph1 unit, while HOMO−5 is an n-orbital of the epoxy oxygen, O2, thus the 5th transition is of $\pi_{Ph1} \rightarrow \pi^*_{CO}$ character, the 6th one is a $n_{O2} \rightarrow \pi^*_{CO}$ type charge transfer (CT) transition.

2.3.2. Substituent effects. As can be seen in Figure 2, the experimental spectra of the methyl derivatives **3a** and **3e** show a close resemblance to the spectrum of the unsubstituted compound **3**, whereas the spectra of the alkoxy derivatives **3b–d** differ markedly: the two strong bands of **3** shift to lower wavelengths and a third intense band appears around 320 nm. The analysis of the theoretical results leads to a plausible explanation.

Although the effect of methyl-substitution on the experimental spectrum is modest, the assignment of the spectrum is somewhat different. The methyl substituent in the Ph2 group induces a shift of the transition corresponding to the 3rd ($\pi_{Ph2} \rightarrow \pi^*_{CO}$) one of **3** to lower energies. Hence, the shoulder at 290 nm is assigned to the 3rd transition of **3**, while the shoulders at 282 and 270 nm likely correspond to the 2nd and 4th transitions of the unsubstituted compound, respectively. In addition, the methyl substitution results in a change in the energy of the $n_{O2} \rightarrow \pi^*_{CO}$ transition (6th of **3**): it shifts to the higher energies, thus the 5th and 6th transitions of **3** are reversed and their quasi-degeneracy is broken.

The influence of the methoxy substituent is even more pronounced. The HOMO, HOMO−1, HOMO−2, and HOMO−3 orbitals, which determine the low-energy part of the spectrum, are strongly perturbed. The introduction of the methoxy substituent into the Ph1 group is accompanied by a decrease in the energy of the $\pi_{Ph1} \rightarrow \pi^*_{CO}$ transition, which is the analogue of the 4th transition of **3**. Due to this shift, the above $\pi \rightarrow \pi^*$ transition of **3b** will be the second in order of increasing energy and the quasi-degeneracy of the 3rd and 4th transitions of **3** is again lifted. The shift manifests in the appearance of a strong peak at 313 nm corresponding to the 4th transition of **3**. Furthermore, the 6th transition of **3b** shifts to lower energies, and thus the 5th and 6th transitions of this molecule will be more separated.

2.4. Stereostructures and CD spectra

The experimental CD spectrum of (−)-**3**, which is shown in Figure 1b, proves that (−)-**3** is identical to the (2*R*,3*S*)-enantiomer since this spectrum agrees with the one obtained for this isomer by Marsman and Wynberg who determined the absolute configuration by chemical correlation.[4] The calculated CD spectrum of (−)-**3** obtained from the theoretically computed wavelengths and rotatory strengths in Table 2, presuming Gaussian band shapes of widths $\sigma = 0.2$ eV,[29] can be seen in Figure 1c. The observed spectra of the substituted compounds are shown in Figure 4.

The source of the chirality in case of *trans*-chalcone epoxides is the strained epoxide ring that involves two stereocenters. Since the epoxide ring is not a chromophoric unit, the Cotton effects in the CD spectra of chalcone epoxides originate from inherently symmetric chromophores that are asymmetrically perturbed by these stereocenters. These chromophore units are the carbonyl group and the chirally fixed phenyl rings of the molecule.

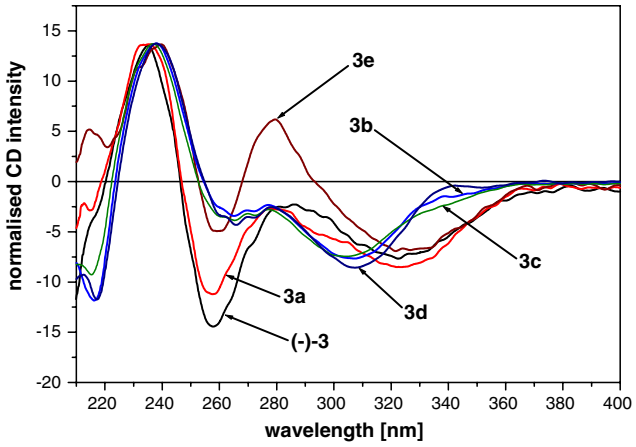

Figure 4. CD-spectra of *trans*-chalcone epoxide (−)-**3** and its substituted derivatives **3a–e**. The spectra are normalized to the same height at the maximum of the highest energy band to facilitate comparison.

2.4.1. The signal of the carbonyl group. In the CD spectrum of (−)-**3**, the lowest-energy transition gives rise to a negative Cotton effect around 320 nm. In case of saturated ketones the sign of this n–π* carbonyl band correlates with the absolute configuration according to the octant rule.[30] For predicting the sign of the carbonyl band of unsaturated ketones modified versions of the octant rule have been proposed, such as the 'helicity rule' for α,β-unsaturated ketones and the 'extended octant rule' for β,γ-unsaturated ones.[31]

To decide if the octant rule applies to the chalcone epoxide, the octant projection diagram of the (2*R*,3*S*)-enantiomer was prepared by rotating the calculated equilibrium structure into the appropriate position. The diagram is shown in Figure 5. The octant rule for such an arrangement predicts a negative Cotton effect, since the chiral disturbance of the carbonyl group arises primarily from the atoms lying in the

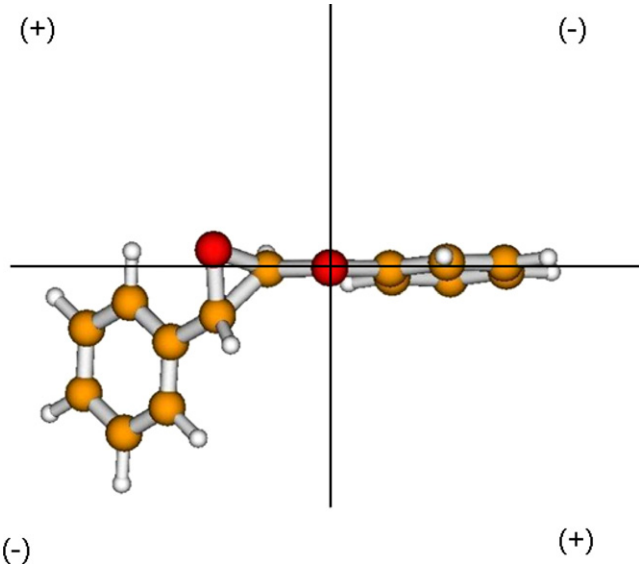

Figure 5. Octant projection diagram for the lowest-energy conformer of *trans*-chalcone epoxide (−)-**3**.

lower back left octant. Consequently, the negative sign of the carbonyl band in the CD spectrum of (2*R*,3*S*)-**3** is in accordance with the octant rule. Thus, the conjugation between the carbonyl group and the phenyl ring, which are quasi-coplanar in our molecule, leads to a red shift of the n–π^* carbonyl band but not to the reversion of its sign.

Since the rotatory strengths of the (2*R*,3*S*)-isomer have been calculated, the absolute configuration can also be obtained by a direct comparison of the signs of the observed and calculated carbonyl signals. The calculated negative rotatory strength confirms the (2*R*,3*S*) configuration of the stereocenters in (−)-**3**.

Comparing the $\lambda > 300$ nm ranges of the CD spectra of the substituted derivatives to that of the unsubstituted compound, noticeable differences can be seen in the spectra of the alkoxy derivatives **3b**–**d**. These spectra contain a band at ~310 nm with a shoulder around 330 nm. The negative signs of these features are in accordance with the sign of the calculated rotatory strengths of the first and second transitions of **3b**. Taking into account the descriptions of the two transitions, the shoulder may be assigned as the 'carbonyl signal'.

2.4.2. The CD-spectra between 220 and 300 nm. In the CD spectrum of (−)-**3**, there is a positive band at 235 nm and a negative one at 259 nm—the latter with two shoulders—in the wavelength range of the strong UV absorption band around 250 nm. They resemble an exciton couplet,[32] while the inflection point between them almost coincides with the maximum of the UV band. If it is a couplet its appearance can be due to the coupling between two singlet transitions—the 5th and 6th in Table 2, which was described qualitatively as a $\pi \rightarrow \pi^*$ excitation of the benzoyl moiety, and as a CT type $n \rightarrow \pi^*$ transition with the involvement of the epoxy and carbonyl unit. It is more likely, however, that the negative band is associated with two pairs of closely lying transitions—3rd and 4th, 5th and 6th—in which the component with the negative rotating power is dominant. In the lower wavelength range of the spectrum, the density of transitions increases substantially, making the assignment of the strong positive band difficult. The calculations suggest that in this feature the contribution of the 12th transition is dominant. This transition, which can be described as a mixture of $\pi_{Ph1} \rightarrow \pi^*_{Ph1}$ and $\pi_{Ph1} \rightarrow \pi^*_{Ph2}$ excitations, has a very high positive rotating power.

In the spectra of **3a**–**d**, derivatives with *ortho*-substituted benzoyl rings, the negative bands around 260 nm are weaker than in the spectrum of the parent compound. Calculations predict a positive band for **3a** and **3b** in the position of the 260 nm negative one of (−)-**3**. The experimental spectra do not show such a dramatic change, but the respective negative bands are much weaker than in the spectrum of the parent compound.

The observed and calculated spectra of **3e**, the derivative with a methyl group in the *o*-position of the Ph2 ring, are in good agreement. The positive band around 280 nm can be assigned to the 3rd and 4th, the negative band around 260 nm to the 5th and 6th transitions.

3. Conclusion

There are three main features in the CD spectrum of the parent compound, a carbonyl band around 320 nm, and two further strong bands, at 260 nm and 235 nm, which can be assigned to the overlapping signals of several transitions. The analogous bands appear in the spectra of derivatives with substituents in the *ortho* and, as reported in our previous papers, in *para*-positions of the aromatic rings, facilitating a simple method for the determination of their absolute configuration. The theoretical calculations with the TD-DFT method led to a plausible assignment of the UV and CD spectra.

4. Experimental

4.1. Instrumentation

Melting points were determined using a Büchi 510 apparatus and are uncorrected. The optical rotations were measured on a Perkin–Elmer 241 polarimeter at 22 °C, while the IR spectra were recorded on a Perkin–Elmer 237 spectrophotometer. NMR spectra were obtained on a Brucker 300 and a Brucker DRX-500 instrument in $CDC1_3$. Mass spectra were obtained on a Varian MAT312 instrument. Analytical and preparative thin layer chromatography was performed on silica gel plates (60 GF-254, Merck), while column chromatography was carried out using 70–230 mesh silica gel (Merck). The shift reagent was $Eu(hfc)_3$ (Aldrich Chem. Co.).

UV–vis absorption spectra of chalcone epoxides were recorded on an Agilent 8453 diode array spectrometer, their CD spectra were recorded on a Jasco J-810 spectropolarimeter. The solvent was of HPLC grade ethanol from Merck.

4.2. Preparation of alkoxymethyl acetophenon, 5c

A solution of the 2-hydroxyacetophenone **4** (7.0 g, 51 mmol) in 15% (m/v) aq KOH (70 ml) was stirred for 2 h. CH_2Cl_2 (70 ml) and Aliquat 336 phase transfer catalyst (5.25 g, 15.6 mmol) were added and stirring was continued for 10 min. Chloromethyl ethyl ether (6.53 g, 69 mmol) was added dropwise and the mixture stirred for 50 min at ambient temperatures. Removal of the organic phase and extraction of the aqueous layer with CH_2Cl_2 (2×20 ml) gave the crude product after drying over Na_2SO_4 and evaporation of the solvent. Flash chromatography with $CHCl_3$ eluent yielded 4.65 g of the pure product **5c** as an oil (47%). ^1H NMR (500 MHz, $CDCl_3$) δ ppm: 1.25 (t, 3H); 2.63 (s, 3H); 3.76 (q, 2H); 5.33 (s, 2H); 7.04 (t, 1H); 7.21 (d, 1H); 7.44 (t, 1H); 7.70 (d, 1H). ^{13}C NMR (300 MHz, $CDCl_3$) δ ppm: 15.22; 31.90; 64.92; 93.32; 115.03; 121.70; 129.21; 130.27; 133.61; 156.70; 200.06. HRMS calcd for $C_{11}H_{14}O_3$ (M^+): 194.0943, found: 194.0955.

4.3. Preparation of chalcones

To a solution of the appropriate acetophenone (36 mmol) in ethanol (10 ml) was added a solution of NaOH (46 mmol) in water (16 ml) and the mixture was stirred at room temperature for 30–40 min. Excess benzaldehyde (37.8 mmol in 10 ml EtOH) was added dropwise and the reaction was monitored by TLC (hexane–EtOAc 10:1). After the disappearance of the acetophenone (4–36 h), water (40 ml) was added and the products extracted with $CHCl_3$ (2×50 ml). The combined extracts were washed with aq HCl (30 ml) and water (2×50 ml). Drying of the extracts over Na_2SO_4 followed by evaporation and flash column chromatography, gave the pure chalcones as an oil, **2a** (90%),[1f] **2b** (68%),[1g] **2c** (67%) **2d** (59%), **2e** (65%).[1c] The data are given only for the novel analogues, **2c** and **2d**.

4.3.1. 2′-*O*-Ethoxymethylchalcone, 2c. Yield: 67% (yellow oil); ^{1}H NMR (500 MHz, $CDCl_3$) δ ppm: 1.20 (t, 3H); 3.71 (q, 2H); 5.28 (s, 2H); 7.08 (t, 1H); 7.23 (d, 1H); 7.32–7.47 (m, 5H); 7.57–7.62 (m, 4H). ^{13}C NMR (500 MHz, $CDCl_3$) δ ppm: 15.25; 64.91; 93.77; 115.51; 122.05; 127.34; 128.54 (2×); 129.11 (2×); 130.25; 130.42; 130.51; 132.81; 135.24; 143.71; 155.88; 193.50. HRMS calcd for $C_{18}H_{18}O_3$ (M^+): 282.1256, found: 282.1264.

4.3.2. 2′-*O*-Isopropylchalcone, 2d. Yield: 59% (yellow oil); ^{1}H NMR (300 MHz, $CDCl_3$) δ ppm: 1.35 (d, 6H); 3.71 (q, 2H); 4.64 (m, 1H); 6.97–7.04 (m, 2H); 7.38–7.67 (m, 9H). ^{13}C NMR (300 MHz, $CDCl_3$) δ ppm: 22.14; 29.70; 71.18; 114.31; 120.62; 127.34; 128.25 (2×); 128.88 (2×); 130.06; 130.47; 130.72; 132.80; 135.31; 142.25; 155.65; 193.05. HRMS calcd for $C_{18}H_{18}O_2$ (M^+): 266.1307, found: 266.1302.

4.4. Epoxidation of chalcones

A solution of chalcone (1.44 mmol) and the chiral catalyst **1** (0.1 mmol) in toluene (3 ml) containing sodium hydroxide (1 ml 20% aq) was treated with 50% *tert*-butylhydroperoxide in decane (0.5 ml, 2.88 mmol) and the mixture stirred at 0–4 °C. After a reaction time of 4–12 h, a new portion of toluene (7 ml) and water (10 ml) were added. The organic phase was washed twice with 10% aq hydrochloric acid (10 ml) and then with (10 ml) water. The organic phase was dried over Na_2CO_3. The crude product obtained after evaporating the solvent was purified by preparative TLC (silica gel, hexane–ethylacetate, 10:1, eluant) to give epoxy ketones **3a**–**e** in pure form.

4.4.1. (2*R*,3*S*)-2,3-Epoxy-1-(2-tolyl)-3-phenylpropan-1-one, 3a. Yield: 52% (yellow oil); $[\alpha]_D^{22} = -166.9$ (*c* 1, CH_2Cl_2); 71% ee; ^{1}H NMR (500 MHz, $CDCl_3$) δ ppm: 2.55 (s, 3H); 4.04 (d, $J = 1.5$ Hz, 1H); 4.10 (d, $J = 1.5$ Hz, 1H); 7.25–7.30 (m, 2H); 7.36–7.44 (m, 6H); 7.68 (d, 1H). HRMS calcd for $C_{16}H_{14}O_2$ (M^+): 238.0994, found: 238.1006.

4.4.2. (2*R*,3*S*)-2,3-Epoxy-1-(2-methoxyphenyl)-3-phenylpropan-1-one, 3b. Yield: 49% (white oil); $[\alpha]_D^{22} = -98.5$ (*c* 1, CH_2Cl_2); 83% ee; ^{1}H NMR (500 MHz, $CDCl_3$) δ ppm: 3.61 (s, 3H); 4.01 (d, $J = 1.5$ Hz, 1H); 4.31 (d, $J = 1.5$ Hz, 1H); 6.93 (d, 1H); 7.05 (t, 1H); 7.36–7.40 (m, 5H); 7.52 (t, 1H); 7.83 (d, 1H). HRMS calcd for $C_{16}H_{14}O_3$ (M^+): 254.0943, found: 254.0940.

4.4.3. (2*R*,3*S*)-2,3-Epoxy-1-(2-ethoxymethyloxyphenyl)-3-phenylpropan-1-one, 3c. Yield: 46% (white crystals); mp: 81–82 °C; $[\alpha]_D^{22} = -102.3$ (*c* 1, CH_2Cl_2); 70% ee; ^{1}H NMR (500 MHz, $CDCl_3$) δ ppm: 1.03 (t, 3H); 3.30 (q, 2H); 4.01 (d, $J = 2$ Hz, 1H); 4.30 (d, $J = 1.5$ Hz, 1H); 4.90 (d, 1H); 4.97 (d, 1H); 7.09 (t, 1H); 7.19 (d, 1H); 7.35–7.41 (m, 5H); 7.49 (t, 1H); 7.81 (d, 1H). HRMS calcd for $C_{18}H_{18}O_4$ (M^+): 298.1205, found: 298.1209.

4.4.4. (2*R*,3*S*)-2,3-Epoxy-1-(2-isopropoxyphenyl)-3-phenylpropan-1-one, 3d. Yield: 53% (yellow crystals); mp: 116–118 °C ; $[\alpha]_D^{22} = -131$ (*c* 1, CH_2Cl_2); 79% ee; ^{1}H NMR (500 MHz, $CDCl_3$) δ ppm: 0.93 (t, 6H); 4.01 (d, $J = 1.5$ Hz, 1H); 4.44 (d, $J = 1.5$ Hz, 1H); 4.57 (m, 1H); 6.93 (d, 1H); 7.01 (t, 1H); 7.33–7.40 (m, 5H); 7.48 (t, 1H); 7.85 (d, 1H). HRMS calcd for $C_{18}H_{18}O_3$ (M^+): 282.1256, found: 282.1260.

4.4.5. (2*R*,3*S*)-2,3-Epoxy-1-phenyl-3-(2-tolyl)-propan-1-one, 3e. Yield: 55% (yellow oil); $[\alpha]_D^{22} = -75.7$ (*c* 1, CH_2Cl_2); 76% ee; ^{1}H NMR (500 MHz, $CDCl_3$) δ ppm: 2.37 (s, 3H); 4.22 (d, $J = 1.5$ Hz, 2H); 7.20 (t, 1H); 7.26–7.28 (m, 2H); 7.34 (t, 1H); 7.51 (t, 2H); 7.64 (t, 1H); 8.05 (d, 1H). HRMS calcd for $C_{16}H_{14}O_2$ (M^+): 238.0994, found: 238.0983.

Acknowledgment

This work was supported by Grants T42546, T42514, and D 48583 from the Hungarian Research Foundation. The authors are grateful to Dr. Thorsten Metzroth (University of Mainz) for his help in the conformational analysis and MP2 calculations.

References

1. (a) Klein, S.; Roberts, S. M. *J. Chem. Soc., Perkin Trans. 1* **2002**, *23*, 2686–2691; (b) Jayaprakash, D.; Kobayashi, Y.; Arai, T.; Hu, Q.-S.; Zheng, X.-F.; Pu, L.; Sasai, H. *J. Mol. Catal. A* **2003**, *196*, 145–149; (c) Geller, T.; Gerlach, A.; Krüger, C. M.; Militzer, H.-C. *Tetrahedron Lett.* **2004**, *45*, 5065–5067; (d) Carrera, G.; Colonna, S.; Meek, A. D.; Ottolina, G.; Roberts, S. M. *Tetrahedron: Asymmetry* **2004**, *15*, 2945–2949; (e) Mathew, S. P.; Gunathilagan, S.; Roberts, S. M.; Blackmond, D. G. *Org. Lett.* **2005**, *7*, 4847–4850; (f) Schuetz, S. A.; Bowman, E. A.; Silvernail, C. M.; Day, V. W.; Belot, J. A. *J. Organomet. Chem.* **2005**, *690*, 1011–1017; (g) Kumamoto, T.; Ebine, K.; Endo, M.; Araki, Y.; Fushimi, Y.; Miyamoto, I.; Ishikawa, T.; Isobe, T.; Fukuda, K. *Heterocycles* **2005**, *66*, 347–359; (h) Lattanzi, A. *Adv. Synth. Catal.* **2006**, *348*, 339–346; (i) Licini, G.; Bonchio, M.; Broxterman, Q. B.; Kaptein, B.; Moretto, A.; Toniolo, C.; Scrimin, P. *Biopolymers.* **2006**, *84*, 97–104; (j) Berkessel, A.; Koch, B.; Toniolo, C.; Rainaldi, M.; Broxterman, Q. B.; Kaptein, B. *Biopolymers.* **2006**, *84*, 90–96; (k) Kee, S.-P.; Gavriiiliidis, A. *J. Mol. Catal. A* **2007**, *263*, 156–162.
2. (a) Porter, M. J.; Skidmore, J. *Chem. Commun.* **2000**, 1215–1225; (b) Daikai, K.; Hayano, T.; Kino, R.; Furuno, H.;

Kagawa, T.; Inanaga, J. *Chirality* **2003**, *15*, 83–88; (c) Ye, J.; Wang, Y.; Liu, R.; Zhang, G.; Zhang, Q.; Chen, J.; Liang, X. *Chem. Commun.* **2003**, *21*, 2714–2715; (d) Bakó, T.; Bakó, P.; Keglevich, Gy.; Bombicz, P.; Kubinyi, M.; Pál, K.; Bodor, S.; Makó, A.; Tőke, L. *Tetrahedron: Asymmetry* **2004**, *15*, 1589–1595; (e) Kumaraswamy, G.; Jena, N.; Sastry, M. N. V.; Rao, G. V.; Ankamma, K. *J. Mol. Catal. A* **2005**, *230*, 59–67; (f) Bakó, P.; Makó, A.; Keglevich, Gy.; Kubinyi, M.; Pál, K. *Tetrahedron: Asymmetry* **2005**, *16*, 1861–1871.

3. (a) Bezuidenhoudt, B. C. B.; Swanepoel, A.; Augustyn, J. A. N.; Ferreira, D. *Tetrahedron Lett.* **1987**, *28*, 4857–4860; (b) Augustyn, J. A. N.; Bezuidenhoudt, B. C. B.; Ferreira, D. *Tetrahedron* **1990**, *46*, 2651–2660; (c) Augustyn, J. A. N.; Bezuidenhoudt, B. C. B.; Swanepoel, A.; Ferreira, D. *Tetrahedron* **1990**, *46*, 4429–4442; (d) van Rensburg, H.; van Heerden, P. S.; Bezuidenhoudt, B. C. B.; Ferreira, D. *Tetrahedron* **1997**, *53*, 14141–14152; (e) Marais, J. P.; Ferreira, D.; Slade, D. *Phytochemistry* **2005**, *66*, 2145–2176.
4. Marsman, B.; Wynberg, H. *J. Org. Chem.* **1979**, *44*, 2312–2314.
5. Moscowitz, A. *Adv. Chem. Phys.* **1962**, *4*, 67–111.
6. (a) Hansen, A. E.; Bouman, T. D. *Adv. Chem. Phys.* **1980**, *44*, 545–644; (b) Hansen, A. E.; Voigt, B.; Rettrup, S.; Bouman, T. D. *Int. J. Quantum Chem.* **1983**, *23*, 595–611.
7. (a) Carnell, M.; Peyerimhoff, S. D.; Breest, A.; Godderz, K. H.; Ochmann, P.; Hormes, J. *Chem. Phys. Lett.* **1991**, *180*, 477–481; (b) Carnell, M.; Peyerimhoff, S. D. *Chem. Phys.* **1994**, *183*, 37–44; (c) Carnell, M.; Grimme, S.; Peyerimhoff, S. D. *Chem. Phys.* **1994**, *179*, 385–394.
8. (a) Pedersen, T. B.; Koch, H.; Ruud, K. *J. Chem. Phys.* **1999**, *110*, 2883–2892; (b) Ruud, K.; Helgaker, T. *Chem. Phys. Lett.* **2002**, *352*, 533–539; (c) Tam, M. C.; Russ, N. J.; Crawford, T. D. *J. Chem. Phys.* **2004**, *121*, 3550–3557; (d) Crawford, T. D.; Owens, L. S.; Tam, M. C.; Schreiner, P. R.; Koch, H. *J. Am. Chem. Soc.* **2005**, *127*, 1368–1369.
9. (a) Furche, F.; Ahlrichs, R.; Wachsmann, C.; Weber, E.; Sobanski, A.; Vogtle, F.; Grimme, S. *J. Am. Chem. Soc.* **2000**, *122*, 1717–1724; (b) Autschbach, J.; Ziegler, T.; van Gisbergen, S. J. A.; Baerends, E. J. *J. Chem. Phys.* **2002**, *116*, 6930–6940; (c) Toyota, S.; Shimasaki, T.; Tanifuji, N.; Wakamatsu, T. *Tetrahedron: Asymmetry* **2003**, *14*, 1623–1629; (d) Pecul, M.; Ruud, K.; Rizzo, A.; Helgaker, T. *J. Phys. Chem. A* **2004**, *108*, 4269–4276; (e) Norman, P.; Ruud, K.; Helgaker, T. *J. Chem. Phys.* **2004**, *120*, 5027–5035; (f) Claps, M.; Parrinello, N.; Saá, C.; Varela, J. A.; Caccamese, S.; Rosini, C. *Tetrahedron: Asymmetry* **2006**, *17*, 1387–1393.
10. Neugebauer, J.; Baerends, E. J.; Nooijen, M.; Autschbach, J. *J. Chem. Phys.* **2005**, *122*, 234305.
11. Nooijen, M. *Int. J. Quantum Chem.* **2006**, *106*, 2489–2510.
12. (a) Chen, W.-P.; Egar, A. L.; Hursthouse, M. B.; Malik, K. M. A.; Mathews, J. E.; Roberts, S. M. *Tetrahedron Lett.* **1998**, *39*, 8495–8498; (b) Arai, S.; Tsuge, H.; Shioiri, T. *Tetrahedron Lett.* **1998**, *39*, 7563–7566; (c) Takagi, R.; Begum, S.; Siraki, A.; Yoneshige, A.; Koyama, K. I.; Ohkata, K. *Heterocycles* **2004**, *64*, 129–141.
13. Stahl, I.; Schomburg, S.; Kalinowski, H. O. *Chem. Ber.* **1984**, *117*, 2247–2260.
14. Yasui, S.; Fujii, M.; Ohno, A. *Bull. Chem. Soc. Jpn.* **1987**, *60*, 4019–4026.
15. Hine, J.; Skoglund, M. J. *J. Org. Chem.* **1982**, *47*, 4758–4766.
16. Cheung, W.-H.; Zheng, S.-L.; Yu, W.-Y.; Zhou, G.-C.; Che, C.-M. *Org. Lett.* **2003**, *5*, 2535–2538.
17. Halgren, A. *J. Comput. Chem.* **1996**, *17*, 490–519.
18. SPARTAN'02, Wavefunction, Irvine, CA, **2002**.
19. Weigend, F.; Häser, M. *Theor. Chem. Acc.* **1997**, *97*, 331–340.
20. Weigend, F.; Häser, M.; Patzelt, H.; Ahlrichs, R. *Chem. Phys. Lett.* **1998**, *294*, 143–152.
21. Ahlrichs, R.; Bär, M.; Häser, M.; Horn, H.; Kölmel, C. *Chem. Phys. Lett.* **1989**, *162*, 165–169.
22. (a) Lee, C. T.; Yang, W. T.; Parr, R. G. *Phys. Rev. B* **1988**, *37*, 785–789; (b) Becke, A. D. *J. Chem. Phys.* **1993**, *98*, 5648–5652.
23. Hariharan, P. C.; Pople, J. A. *Theor. Chim. Acta* **1973**, *28*, 213–222.
24. Autschbach, J.; Ziegler, T. *J. Chem. Phys.* **2002**, *116*, 891–896.
25. (a) Miertus, S.; Scrocco, E.; Tomasi, J. *Chem. Phys.* **1981**, *55*, 117–129; (b) Mennucci, B.; Tomasi, J. *J. Chem. Phys.* **1997**, *106*, 5151–5158.
26. Frisch, M. J.; Trucks, G. W.; Schlegel, H. B. GAUSSIAN *03, Revision B.01*; Gaussian: Pittsburgh, PA, 2003.
27. Borst, D. R.; Pratt, D. W. *J. Chem. Phys.* **2000**, *113*, 3658–3669.
28. Molina, V.; Merchán, M. *J. Phys. Chem. A* **2001**, *105*, 3745–3751.
29. Mc Cann, D. M.; Stephens, P. J. *J. Org. Chem.* **2006**, *71*, 6074–6098.
30. Lightner, D. A. In *Circular Dichroism, Principles and Applications*; Berova, N., Nakanishi, K., Woody, R., Eds.; W. Wiley-VCH: New York, 2000; pp 261–303.
31. Kirk, D. N. *Tetrahedron* **1986**, *42*, 777–818.
32. Berova, N.; Nakanishi, K. In *Circular Dichroism, Principles and Applications*; Berova, N., Nakanishi, K., Woody, R., Eds.; W. Wiley-VCH: New York, 2000; pp 337–382.